IEEJ Journal of Industry Applications
Vol.3 No.6 pp.446–454 DOI: 10.1541/ieejjia.3.446

Paper

Size Reduction of DC-DC Converter using Flying Capacitor Topology with Small Capacitance

Asmarashid Bin Ponniran* Student Member, Koichi Matsuura* Non-member
Koji Orikawa* Member, Jun-ichi Itoh*a) Member

(Manuscript received Dec. 24, 2013, revised May 14, 2014)

The purpose of the present paper is to analyze the input inductor design and to establish the relationship between the capacitance of the flying capacitor and the output voltage ripple in order to reduce the size and weight of the flying capacitor DC-DC boost converter (FCBC). The inductance of the input inductor is designed by considering the maximum input current ripple, and the experimental results are used to confirm that the input current ripple is within the designed value. Furthermore, according to the design specifications, the required inductance of an input inductor is approximately 25% of that of a conventional two-level DC-DC boost converter, and the required inductor core volume is approximately 35% of that of a conventional two-level DC-DC boost converter. Moreover, the capacitance of the flying capacitor and the output voltage ripple are confirmed to be independent of each other. Theoretically, this is because the time constant of the output capacitance and the output resistance of the FCBC is larger than the switching period of the switching frequency. This finding is confirmed by the simulation and experimental results of the present study. On the basis of this finding, the capacitance of the flying capacitor can be estimated and designed without considering the output voltage ripple. Moreover, the achieved maximum efficiency of the designed FCBC is 98.5% of the output power at 1 kW.

Keywords: inductor size, flying capacitor, output voltage ripple, flying capacitor boost chopper

1. Introduction

In general, as a power converter, the DC-DC boost converter is important in high-power-capacity applications, such as solar electric systems and electric vehicle systems. These types of applications typically demand high conversion efficiency with low weight, volume, and cost of the converter. Nevertheless, if a conventional DC-DC boost converter is considered, the bulkiness of the input inductor must be taken into consideration because a typical conventional DC-DC boost converter requires large inductors for energy storage, especially for continuous-current-mode operation of the input current. Although conventional DC-DC boost converters are evolving due to these drawbacks, the flying capacitor DC-DC boost converter (FCBC) has become a possible option. The FCBC with an input inductor has several advantages over a conventional DC-DC boost converter. The FCBC requires only a small input inductor and the suppression of an input inrush current due to the existing of an input inductor compared to a conventional FCBC without an input inductor [(1)–(4)].

In addition, a number of researchers have reported that interleaved circuit topologies can be considered for conventional DC-DC boost converters. As a result, the input current can be reduced based on the number of interleaved circuits. Consequently, the inductance and core volume of the input inductors can be reduced [(5)–(9)]. Moreover, by considering multilevel structure topologies on the FCBC, the inductance and core volume of the input inductors can also be reduced [(1)–(4)]. However, the interleaved circuit topology and multilevel circuit structure introduce circuit complexity. Furthermore, such topologies require additional inductors, capacitors, and switching devices, as well as other components and devices. Nevertheless, if a very-high-efficiency DC-DC boost converter is critical, regardless of size and weight, such topologies might be an option [(1)(4)–(9)].

Therefore, for single-phase operation and simplicity of the converter circuit, the FCBC offers a good option due to the need for fewer passive components and switching devices. In addition, by considering appropriate designs of the passive components and devices, the sizes and volumes of the components and devices can be minimized.

As in the case of a conventional DC-DC boost converter, the output voltage in the FCBC can be controlled by controlling the duty ratio of the switching signals. One important feature of the FCBC is that the boost-up energy is transferred from the flying capacitor to the output side, which means that the input inductor can be designed with small inductance and a reduced inductor core volume [(1)(4)(10)]. Consequently, the overall size and weight of the input inductor can be greatly reduced as compared to a conventional DC-DC boost converter [(3)(10)]. Moreover, the power loss in terms of copper loss is also reduced as a result of fewer winding of the input inductor. Generally, passive components and devices in the FCBC,

a) Correspondence to: Jun-ichi Itoh. E-mail: itoh@vos.nagaokaut.ac.jp
* Nagaoka University of Technology
1603-1, Kamitomioka-machi, Nagaoka, Niigata 940-2188, Japan

i.e., the input inductor, the flying capacitor, and the output capacitor, must be designed correctly because these components will have a significant impact on converter operation and efficiency. However, this has not been clarified in previous studies [1]–[3][10]–[12].

Moreover, establishing the relationship between the capacitance of the flying capacitor and the output voltage ripple is also important. Unfortunately, this has not been discussed in other studies [1][3][4][13][14]. Converter circuit components/devices and electrical parameters are significantly related. Therefore, procedures for device estimation and design must be established. Generally, the output voltage ripple should be considered as a factor that influences the estimation of the capacitance of the flying capacitor in the FCBC [15][16]. Hence, the parametric relationship between the capacitance of the flying capacitor and the output capacitance from the output voltage ripple must to be analyzed.

In the present paper, an FCBC is proposed considering a small capacitance of the flying capacitor in order to reduce the size of the power converter. Principally, a small capacitance of the flying capacitor causes a large voltage ripple across the flying capacitor. In contrast, the voltage stress increases when a small capacitance of the flying capacitor is used. However, low-power-loss and high-voltage power devices, such as SiC-MOSFETs, have recently been developed. Thus, downsizing is a higher priority than the use of low-voltage-stress switching devices. Moreover, ideally, the voltage stress of the switching devices in the FCBC becomes half that of a two-level DC-DC boost converter. Based on this argument, a small capacitance of the flying capacitor in the FCBC is possible to be considered.

Moreover, the discussion is focused on issues related to the input inductor and flying capacitor. In particular, the authors focus on the input inductor design and establishing the relationship between the capacitance of the flying capacitor and the output voltage ripple.

First, the principle of the FCBC is described. Then, the input inductor design in terms of inductance and inductor core volume is discussed. The parametric relationship between the flying capacitor and output capacitor is discussed considering the output voltage ripple. Experimental and simulation results are analyzed and discussed in order to confirm the validity of the design parameters.

2. Principle of the FCBC

Figure 1(a) shows a conventional DC-DC boost converter. In a conventional DC-DC boost converter, the boost input inductor volume is large. Figure 1(b) shows a three-level FCBC with a function for output voltage control and unidirectional operation. Basically, the FCBC consists of two diodes, two switches (MOSFET), an input inductor L, a flying capacitor C_{fc}, and an output capacitor C_{out}. The input inductor allows the output voltage of the FCBC to be controlled independently by controlling the duty ratio D. In addition, if the input inductor is not considered, the maximum output voltage is double the input voltage V_{in}. The relationship between V_{in} and the output voltage V_{out} is expressed as follows:

$$V_{out} = \beta V_{in} \quad \cdots\cdots (1)$$

where the boost ratio β is expressed as

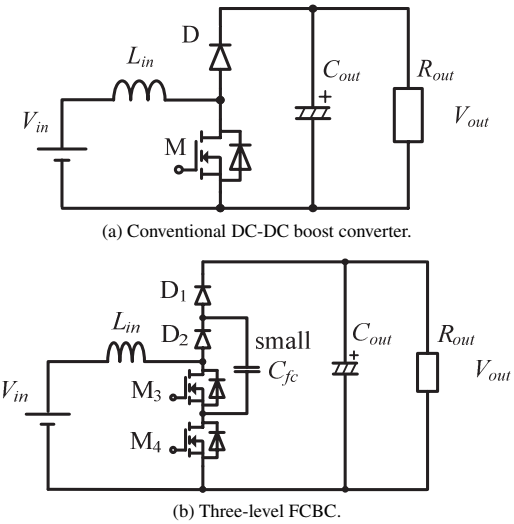

Fig. 1. DC-DC boost converters

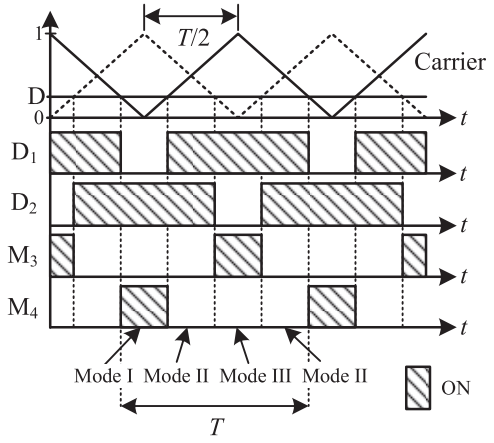

Fig. 2. Switching pattern of the three-level FCBC

$$\beta = \frac{1}{1 - D} \quad \cdots\cdots (2)$$

Figure 2 shows the switching patterns of the FCBC. The switching signal is generated by two carrier signals with half the switching period T delay between the signals. Half of the switching period T delay is needed in order to balance the charging and discharging times of the input inductor in one switching period T. The charging time of the input inductor is determined by the duty ratio D and both carrier signals.

In the FCBC, the duty ratio D is a value in the range of $0 \leq D \leq 1$. If the duty ratio D is set at 0.25, meaning that only 25% of the switching period T is activated. If the FCBC topology is referenced, M_3 and M_4 will receive only ON pulse widths at 25% of the switching period T. Meanwhile, the D_1 and D_2 pulse widths are opposite the M_4 and M_3 pulses width, respectively, as shown in Fig. 2.

Figure 3 shows the operation mode of the FCBC in circuit diagram form. Table 1 summarizes the operation mode and the range of β in the FCBC. The maximum required output voltage of the three-level FCBC in the present paper is twice that of the input voltage. Therefore, only the boost ratio in the range of $0 < \beta \leq 2$ is considered.

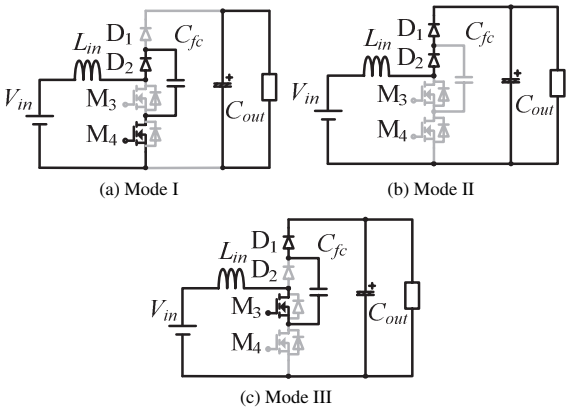

Fig. 3. Operation modes of three-level FCBC

Table 1. Operation mode and boost ratio

Modes of operation	Boost ratio, β
(I), (II), and (III)	$0 < \beta \leq 2$

3. Inductor Design

In this section, the inductor design principle is discussed. The parameters of the FCBC circuit are determined according to the specifications shown in Table 2. Note that the inductor design is discussed under the assumption of a constant flying capacitor voltage. The validity of this assumption is discussed in Sect. 5.

3.1 Inductance of an Input Inductor In order to determine the appropriate inductance of an input inductor L, the desired inductor current ripple ΔI_L is required. For design purposes, it is useful to express the inductance of the input inductor L in terms of the desired inductor current ripple ΔI_L. Ideal characteristics of the switching devices are considered, whereby ripples on the output voltage V_{out} and flying capacitor voltage V_{fc} are ignored due to the independent relationship between the inductor current ripple and capacitance variation of the flying capacitor, as discussed in Sect. 5.3. Generally, the inductance of an input inductor L can be designed by considering the inductor current ripple ΔI_L as expressed as follows:

$$\Delta I_L = V_L \frac{T_L}{L} \quad \cdots\cdots (3)$$

where T_L is the charging time of the inductance of an input inductor, and V_L is the inductor voltage. The inductor current ripple is maximum when the product of T_L and V_L is maximum, as expressed by Eq. (3).

In a conventional DC-DC boost converter, the maximum inductor current ripple occurs when the duty ratio D is 0.5 (β = 2). Under this condition, the charging time of the input inductor becomes half the switching period T, and the inductor voltage is equal to half the output voltage V_{out}. Therefore, the inductance of an input inductor $L_{conventional}$ for a conventional DC-DC boost converter can be expressed as follows:

$$L_{conventional} = \frac{V_{out}}{2} \frac{T}{2} \frac{1}{\Delta I_L} \quad \cdots\cdots (4)$$

In the FCBC, the maximum inductor current ripple occurs for duty ratios of 0.25 (β = 1.33) and 0.75 (β = 4). Figure 4 shows the relationship between the product of T_L and V_L and

Table 2. FCBC Specifications

Parameters	Value
Input voltage V_{in}	262.5 V
Output voltage V_o	350 V
Output power P	1 kW
Inductor/Input current I_{in}	4.24 A
Switching frequency f_{sw}	100 kHz

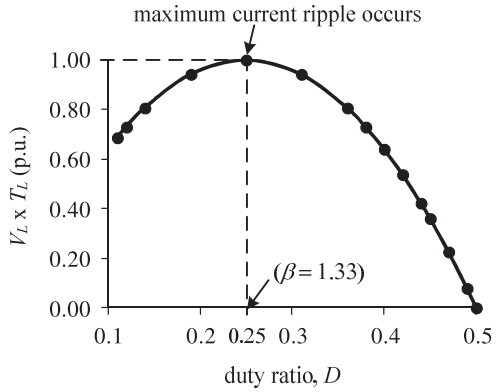

Fig. 4. Relationship between $V_L \times T_L$ (p.u.) and duty ratio D

the duty ratio D in the FCBC. Hence, the inductance of an input inductor L_{FCBC} in terms of the desired inductor current ripple ΔI_L can be expressed as follows:

$$L_{FCBC} = \frac{V_{out}}{4} \frac{T}{4} \frac{1}{\Delta I_L} \quad \cdots\cdots (5)$$

Referring to Eq. (5), the inductor voltage in the FCBC becomes half that of a conventional DC-DC boost converter or a quarter of the output voltage V_{out}. Meanwhile, the charging time of the input inductor in the FCBC becomes half that of a conventional DC-DC boost converter or one quarter of the switching period T.

By considering an FCBC and a conventional DC-DC boost converter having the same output voltage, switching frequency and inductor current ripple ΔI_L, the ratio of the inductances of the input inductor between the FCBC and the conventional DC-DC boost converter can be expressed as follows:

$$\frac{L_{FCBC}}{L_{conventional}} = 0.25 \quad \cdots\cdots (6)$$

Thus, referring to Eq. (6), the FCBC requires approximately 25% of the inductance of an input inductor, as compared to the conventional DC-DC boost converter, as shown in Fig. 1(a).

Therefore, the inductance of an input inductor can greatly be reduced for the FCBC topology [4]. Theoretically, the inductance of an input inductor is proportional to the number of windings. Therefore, the copper loss of an input inductor is also reduced.

3.2 Inductor Core Volume The core volume of an input inductor is discussed based on the area product theory [17]. In this section, the input inductor core volumes for the FCBC and conventional DC-DC boost converters are compared. The inductor core volume *Vol* as a function of constant K_{vol} and the area product A_p can be expressed as follows [17]:

$$Vol = K_{vol}A_p{}^{0.75} = K_{vol}\left[\frac{2W\left(10^4\right)}{B_m J K_u}\right]^{0.75} \quad \cdots\cdots\cdots (7)$$

where B_m is a flux density. Moreover, the energy-handling capability of an inductor core W is related to the area product A_p. The energy-handling capability of an inductor core W can be expressed as follows:

$$W = \frac{1}{2}L \times I^2 \quad \cdots\cdots\cdots\cdots\cdots\cdots\cdots\cdots\cdots\cdots (8)$$

where I is a maximum inductor current.

The inductor core volume Vol can be estimated by considering the energy required for an inductor, as expressed by Eq. (8). Thus, the inductance required by the FCBC is approximately 25% of that required by the conventional DC-DC boost converter. Furthermore, Eq. (8) can also be expressed by the following equations for the FCBC and conventional DC-DC boost converter, respectively:

$$W_{FCBC} = \frac{1}{2}L_{FCBC} \times I^2 = \frac{1}{2}\left(L_{conventional} \times 25\%\right) \times I^2 \quad \cdots\cdots\cdots\cdots\cdots (9)$$

$$W_{conventional} = \frac{1}{2}L_{conventional} \times I^2 \quad \cdots\cdots\cdots\cdots\cdots (10)$$

If the inductance $L_{conventional}$ of a conventional DC-DC boost converter is considered as a reference, the required input inductor core volume of the FCBC is approximately 35% of that of the conventional DC-DC boost converter, as expressed by the following equations:

$$\frac{Vol_{FCBC}}{Vol_{conventional}} = \left(\frac{W_{conventional}}{W_{FCBC}}\right)^{0.75} \quad \cdots\cdots\cdots\cdots\cdots (11)$$

$$Vol_{FCBC} = 35\% \times Vol_{conventional} \quad \cdots\cdots\cdots\cdots\cdots (12)$$

Thus, not only is the inductance reduced, but the inductor core volume is also greatly reduced. Consequently, the overall size and weight of the converter are reduced.

4. Relationship between the Capacitance of the Flying Capacitor and the Output Voltage Ripple

Principally, the time constant $R_{out}C_{out}$, which consists of the output resistance R_{out} and output capacitance C_{out}, can be considered in order to establish the relationship between the capacitance of the flying capacitor and the output voltage ripple. Based on observations, if the output voltage ripple is always constant, even though the capacitance of the flying capacitor varies, the time constant $R_{out}C_{out}$ should be greater than the switching period $1/f_{sw}$, as expressed by Eq. (13). Meanwhile, if the output voltage ripple varies depending on the capacitance variation of the flying capacitor, the time constant $R_{out}C_{out}$ should be either equal to or less than the switching period $1/f_{sw}$. This principle can be proven mathematically in order to establish whether the relationship between the capacitance of the flying capacitor and the output voltage ripple is independent or dependent. Moreover, the time constant $R_{out}C_{out}$ can be expressed as a function of the output voltage and output power. Therefore, in order to estimate and design the capacitance of the flying capacitor without considering the output voltage ripple, the following equation should be satisfied:

$$R_{out}C_{out} = \frac{V_{out}^2}{P}C_{out} > \frac{1}{f_{sw}} \quad \cdots\cdots\cdots\cdots\cdots\cdots (13)$$

Table 3. Time constant and switching period

Output Capacitance C_{out}	Output Resistance R_{out}	Time Constant $R_{out}C_{out}$	Switching Period $1/f_{sw} = T$
1.5 µF	110 Ω	165 µs	10 µs
6 µF		660 µs	
9 µF		990 µs	

Table 4. Charging and discharging states of the input inductor, the flying capacitor, and the output capacitor according to the operation mode of the FCBC

Operation Mode	Input Inductance (L)	Capacitance of the Flying Capacitor (C_{fc})	Output Capacitance (C_{out})
Mode I	charging	charging	discharging
Mode II	discharging	unchanged	charging
Mode III	charging	discharging	charging
Mode II	discharging	unchanged	charging

Note: 1) 'charging'/'discharging' = component is either in charging or discharging conditions. 2) 'unchanged' = component is not in charging or not in discharging conditions.

Based on the simulation and experimental setup, three output capacitances and an output resistance are selected, as shown in Table 3. The switching frequency f_{sw} is set to 100 kHz, which is equivalent to a switching period of 10 μs. Referring to Table 3, it is obvious that all of the time constants $R_{out}C_{out}$ for the numerous output capacitances are greater than the switching period T. This condition is in agreement with Eq. (13). Therefore, the output voltage should be constant. Furthermore, the minimum time constant $R_{out}C_{out}$ for these three conditions is 16.5 times greater than the switching period T. Thus, based on this analysis, the time constant $R_{out}C_{out}$ is always greater than the switching period T as expressed by Eq. (13). This condition leads to the capacitance of the flying capacitor and the output voltage ripple always being independent of each other.

Theoretically, the peak-to-peak measurement of the output voltage ripple of a conventional DC-DC boost converter can be calculated by referring to the output capacitor current waveform, whereby the change in the output capacitor charge Q must be considered [15][16]. This principle can also be considered in order to establish the relationship between the capacitance of the flying capacitor and the output voltage ripple. Table 4 shows the charging and discharging conditions of the passive components/devices, i.e., the input inductor, flying capacitor, and output capacitor according to the operation mode, as shown in Fig. 3.

In order to clarify the charging and discharging conditions of the output capacitor, the converter operation modes shown in Fig. 3 are referenced. By referring to the operation modes shown in Fig. 3, the output capacitor only discharges during Mode I and charges during Modes II and III. Hence, the total charge Q_{total} from these charging and discharging processes for one switching period is equal to zero. This condition can

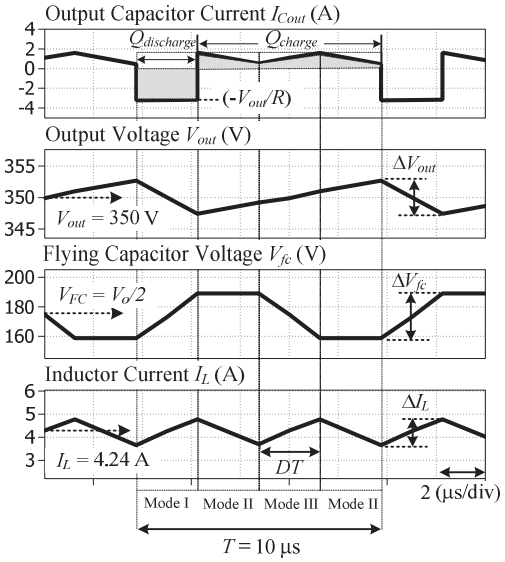

Fig. 5. Simulation waveforms of the output capacitor current, the output voltage, the flying capacitor voltage, and the inductor current

be expressed as follows:

$$Q_{charge} = Q_{discharge} \cdots\cdots (14)$$

Figure 5 shows the simulation results for the waveforms of the output capacitor current, I_{Cout}, the output voltage, V_{out}, the flying capacitor voltage, V_{fc}, and the inductor current, I_L. The specifications of this simulation condition are as follows: output voltage, V_{out} = 350 V, input voltage, V_{in} = 262.5 V, output capacitance, C_{out} = 1.5 μF, capacitance of the flying capacitor, C_{fc} = 0.35 μF, and flying capacitor voltage, $V_{fc} = V_{out}/2$. These simulation results indicate that the peak-to-peak output voltage ripple can be determined by referring to the output capacitor current waveform, as shown in Fig. 5. The change in the output capacitor charge can be calculated as follows [15][16]:

$$\left|\Delta Q_{discharge}\right| = \left(\frac{V_{out}}{R_{out}}\right) DT = C_{out}\Delta V_{out} \cdots\cdots (15)$$

By considering this principle, the output capacitance C_{out} can be estimated in terms of the output voltage ripple ΔV_{out} in the FCBC. Based on Eq. (15), the output voltage ripple ΔV_{out} can be expressed as follows:

$$\Delta V_{out} = \frac{V_{out} D}{R_{out} C_{out} f_{sw}} \cdots\cdots (16)$$

If the boost ratio β and output power P_{out} are considered, Eq. (16) can be rewritten as follows:

$$\Delta V_{out} = \frac{P_{out}(\beta - 1)}{\beta V_{out} C_{out} f_{sw}} \cdots\cdots (17)$$

Based on Eq. (17), the output voltage ripple is proportional to the output power and inversely proportional to the output voltage, the output capacitor, and the switching frequency.

Thus, based on Eq. (17), the capacitance of the flying capacitor and the output voltage ripple are independent. This finding is confirmed by the simulation and experimental results. Therefore, it is confirmed that the capacitance of the flying capacitor can be estimated without relying on the output capacitance or output voltage ripple.

Table 5. Specifications of the simulation and experiment

Specification	Value
Input Voltage V_{in}	262.5 V
Output Voltage V_o	350 V
Output power P_{out}	1 kW
Input current I_{in}	4.24 A
Switching frequency f_{sw}	100 kHz
Duty ratio D	0.25
Input inductance L	200 μH
Capacitance of the flying capacitor C_{fc}	0.35 μF
Output capacitance C_{out}	1.5 μF
Maximum inductor current ripple $\Delta I_{L\text{-}max}$	1.1 A
MOSFET	IRFB4229PBF
SiC Schottky Diode	IDW30G65C5

Table 6. Specifications of the output voltage ripple measurement

Parameters	Value
Output capacitance C_{out}	1.5, 6, 9 μF
Capacitance of the flying capacitor C_{fc}	0.11, 0.35, 0.6, 1.1 μF
Output resistance R_{out}	110 Ω
Duty ratio D	0.25

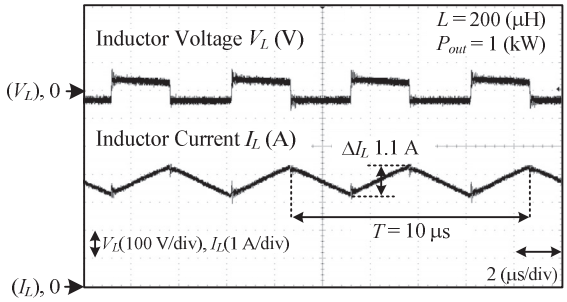

Fig. 6. Experimental waveforms of the inductor voltage and inductor current

5. Experimental Results

In this section, the experimental results and experiment specifications are shown. The details of the experiment specifications are depicted in Table 5. Practically, the selected inductance of an input inductor is 200 μH, which is based on the design principle, as described in Sect. 3. The maximum output power for the conditions of the experiment and the simulation is 1 kW. However, Table 6 also lists the experiment specifications for the observation of the relationship between the capacitance of the flying capacitor and the output voltage ripple.

5.1 Input Inductor Design and Inductor Current Ripple Table 5 lists the experiment specifications. For the design specifications of this prototype, the maximum inductor current ripple, $\Delta I_{L\text{-}max}$, is designed at 1.1 A, as expressed by Eq. (5). Moreover, based on the experimental results, the inductor current ripple is 1.1 A, as shown in Fig. 6. Therefore, the simulation and experimental results are in good agreement, and the inductor current ripple design is confirmed. However, the potential for an unbalanced flying capacitor voltage must be considered for the stable operation of the converter [11][18]–[20].

The inductance and core volume of the input inductor are designed by considering the maximum inductor current ripple as expressed by Eqs. (5) and (12). Theoretically, if the same specifications of the inductor design are considered, the conventional boost DC-DC converter requires an inductance of the input inductor of approximately 800 μH, whereas the FCBC requires an inductance of only approximately 200 μH. Moreover, the copper loss is reduced due to the small inductance of the input inductor. Hence, the FCBC needs only approximately 25% and 35% of an inductance and an inductor core volume of the input inductor, respectively compared to the conventional DC-DC boost converter. Therefore, the reductions in the inductance and inductor core volume of the input inductor are reflected in the reduction of the size and weight of the converter.

5.2 Relationship between the Capacitance of the Flying Capacitor and the Output Voltage Ripple In this section, only the conditions with an output capacitance of 1.5 μF and several capacitances of the flying capacitor is considered in the discussion of the relationship between the capacitance of the flying capacitor and the output voltage ripple, as shown in Fig. 7.

Figure 7 shows the details of the experimental waveforms of the output voltage ripple for an output capacitance of 1.5 μF and various capacitances of the flying capacitor, i.e., 1.1 μF, 0.6 μF, 0.35 μF, and 0.11 μF, respectively. Table 6 lists the specifications of the experiment. In this prototype, film capacitors are used for the output capacitor and the flying capacitor. The experimental results confirm that the peak-to-peak output voltage ripple is 5.6 V for all capacitances of the flying capacitor, because the capacitance of the flying capacitor and the output voltage ripple are independent, as indicated by Eq. (16).

Figure 8 shows a summary of the experimental results of the relationship between the capacitance of the flying capacitor and the output voltage ripple with a fixed output capacitance and various capacitances of the flying capacitor. Table 6 lists the experiment specifications. In order to clarify this phenomenon, small output capacitances (1.5 μF, 6 μF, and 9 μF) and small capacitances of the flying capacitor (0.11 μF, 0.35 μF, 0.6 μF, and 1.1 μF) are selected. The output voltage ripple is confirmed to remain unchanged with respect to the capacitance variation of the flying capacitor, as shown in Fig. 8.

Therefore, these experimental results indicate that the capacitance of the flying capacitor and the output voltage ripple are independent of each other. Hence, the capacitance of the flying capacitor can be estimated without considering the output voltage ripple, as indicated by Eqs. (16) and (17). However, due to the influence of parasitic components and the ESR of the output capacitor, the measured output voltage ripples differ slightly from the simulation results. The errors between the simulation and experimental results are 0.3 V, 0.05 V, and 0.06 V for output capacitances of 1.5 μF, 6 μF and 9 μF, respectively, as shown in Table 7.

5.3 Relationship between the Inductor Current Ripple and the Flying Capacitor Voltage Ripple for Various Capacitances of the Flying Capacitor Figure 9 shows the relationship between the inductor current ripple and the flying capacitor voltage ripple for various capacitances of the flying capacitor, i.e., 1.1 μF, 0.6 μF, 0.35 μF, and 0.11 μF. Based on these relationships, the inductor current ripple is confirmed to remain unchanged with regard to the capacitance variation of the flying capacitor. The flying capacitor voltage ripple depends on the capacitance variation of the flying capacitor, where the flying capacitor voltage ripple becomes high when a small capacitance of the flying capacitor is selected. For further observation, the experimental waveforms of the inductor current ripple and flying capacitor voltage ripple are referenced in order to describe the relationship between the inductor current ripple and the capacitance variation of the flying capacitor, as shown in Fig. 7. Therefore, based on these experimental results, the inductor current

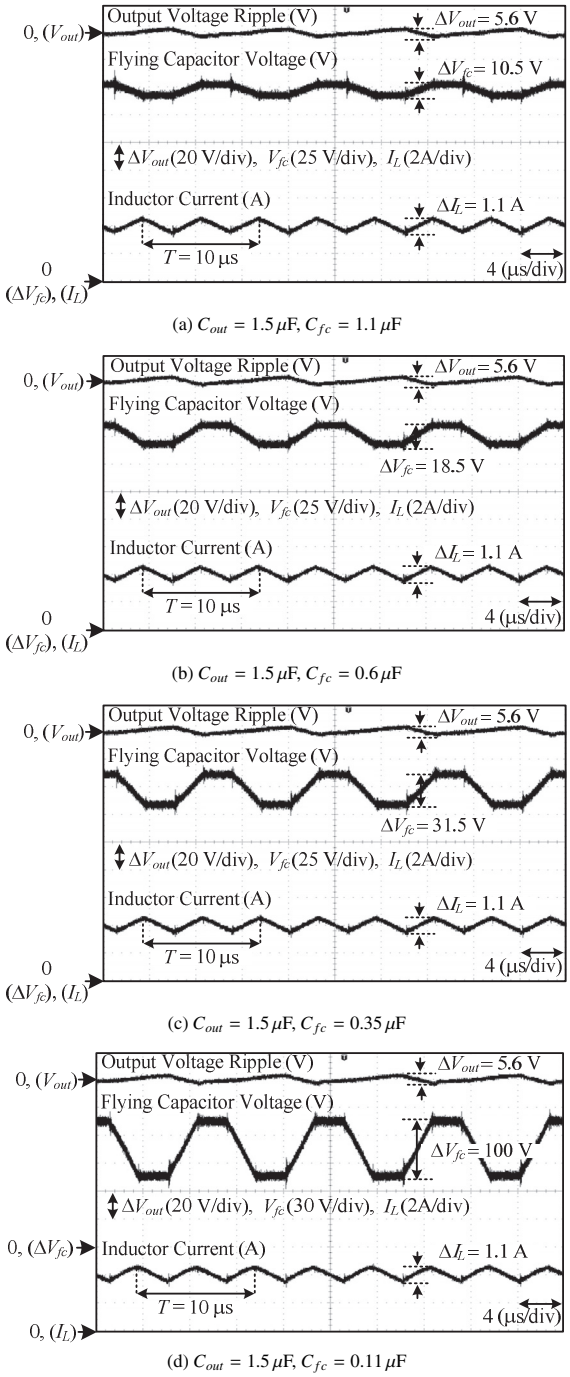

Fig. 7. Experimental waveforms of the output voltage, the flying capacitor voltage, and the inductor current

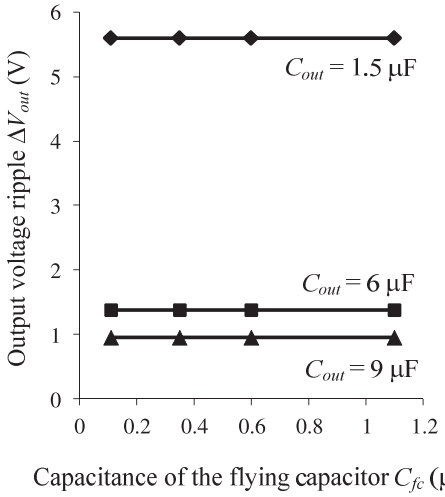

Fig. 8. Relationship between the capacitance of the flying capacitor C_{fc} and the output voltage ripple ΔV_{out}

Table 7. Error ratio between the simulation and experimental results for the output voltage ripple

Output Capacitance C_{out}	Capacitance of the Flying Capacitor C_{fc}	Error (between simulation and experimental results)
1.5 μF	0.11 μF	0.3 V
	0.35 μF	
	0.6 μF	
	1.1 μF	
6 μF	0.11 μF	0.05 V
	0.35 μF	
	0.6 μF	
	1.1 μF	
9 μF	0.11 μF	0.06 V
	0.35 μF	
	0.6 μF	
	1.1 μF	

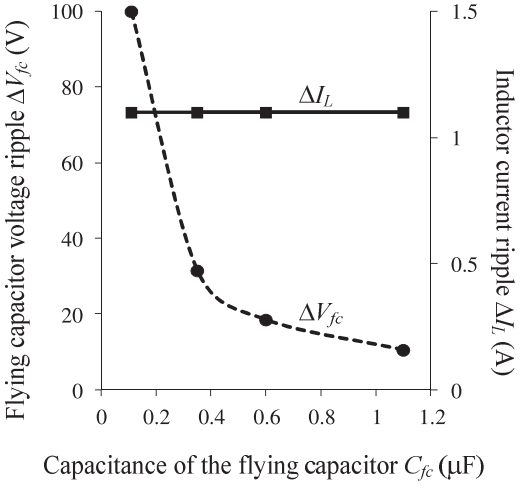

Fig. 9. Relationship between the flying capacitor voltage ripple and the inductor current ripple with the capacitances of the flying capacitor

ripple and capacitance variation of the flying capacitor are independent of each other. The reason for this condition is that the inductor current ripple is dominated by the difference in

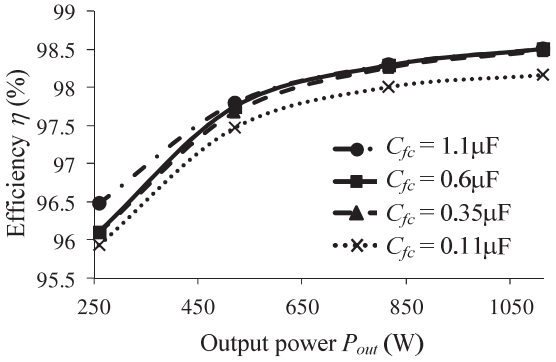

Fig. 10. Relationship between the converter efficiency characteristics and the capacitance variation of the flying capacitor

voltage between the input and output voltages in Mode II, as shown in Fig. 3. As a result, the inductance of an input inductor can be estimated without considering the voltage ripple on the flying capacitor, as described in Sect. 3.

5.4 Converter Efficiency for Several Output Power Levels Figure 10 shows the converter efficiency characteristics. Several output power levels are considered for these experimental results. The output voltage is fixed at 350 V. Several capacitances of the flying capacitor are considered for the efficiency measurement of the constructed prototype circuit. The achieved maximum efficiency is 98.5% for an output power of 1 kW. During this achieved maximum efficiency condition, the capacitances of the flying capacitor are 1.1 μF and 0.6 μF. Moreover, for the same output power condition and a capacitance of the flying capacitor of 0.11 μF, the efficiency is decreased to 98.2% due to the high value of the ESR of the capacitor, as compared to that of the other flying capacitors. Based on these efficiency characteristics, the converter efficiency decreases when the output power is decreasing, as shown in Fig. 10.

5.5 Power Loss Analysis based on Output Power Levels The distribution of the converter power losses is analyzed based on the converter output power. The power losses are distributed into seven parts, i.e., diode conduction loss, MOSFET conduction loss, MOSFET switching loss, inductor copper loss, equivalent series resistance (ESR) loss of the flying capacitor and the output capacitor, no-load loss, and other losses. Moreover, due to the complexity of the estimation of the power losses, other losses such as wiring loss, iron loss, and ringing loss are included in the 'other losses' category, as shown in Fig. 11. In addition, the diode reverse-recovery loss is not considered in the present paper because SiC Schottky barrier diodes without reverse-recovery loss are used in the prototype circuit.

Figure 11 shows the details of a power loss distribution of the FCBC for several output power levels for a capacitance of the flying capacitor of 1.1 μF and an output capacitance of 6 μF are considered. The total power loss of 100% is based on the total power loss when the converter power is increased at 1 kW. Hence, the total power loss is considered as a reference for this power loss distribution analysis.

Based on this power loss distribution analysis, one of the major power losses is dominated by the diode conduction loss for converter power levels of 1 kW and 800 W. However, it

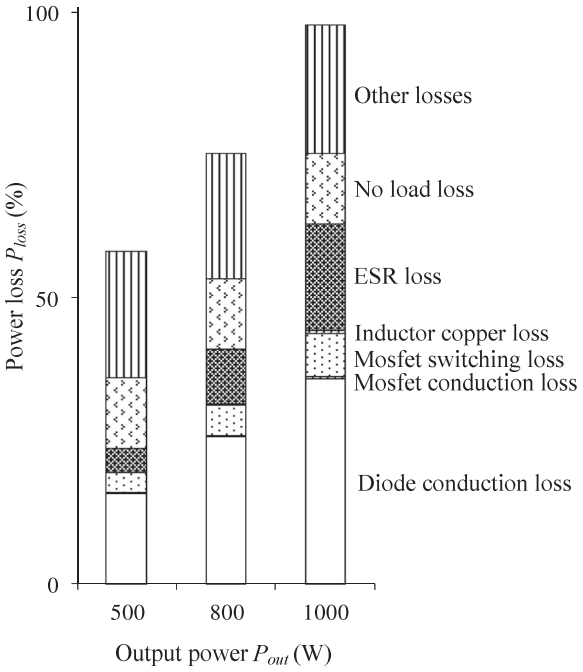

Fig. 11. Converter loss distribution when the capacitance of the flying capacitor is 1.1 μF

was dominated by the 'other losses' for a converter power level of 500 W. The inductor copper loss was the lowest component of the total power loss. Moreover, at output power levels of 1 kW and 800 W, 'other losses' were the second largest power losses, followed by the diode conduction loss for a converter power level of 500 W.

Based on this power loss analysis, the inductor copper loss is small due to smaller number of inductor windings. Moreover, MOSFET conduction loss is considered to be small due to the low input current with regard to the small boost ratio. If the boost ratio is high, the input current becomes high. As a result, the conduction loss of the MOSFET becomes high.

Since one of the major power losses is associated with the diodes, low-on-voltage diodes must be considered in order to reduce the conduction loss of the diodes. Moreover, the conduction loss in the flying capacitor is considered to be high due to the high value of the ESR. Therefore, a low ESR for the flying capacitors must be selected in order to reduce the flying capacitor conduction loss. In order to reduce the power loss in the MOSFETs when a high boost ratio is considered, low-on-resistance MOSFETs must be selected. As an option, the on-resistance can be further reduced by connecting the MOSFETs in parallel connection. Therefore, by considering these available options, the overall converter efficiency can be improved further.

6. Conclusion

In the present paper, the authors examined an FCBC with a small-capacitance flying capacitor considering the output voltage ripple. Moreover, the authors discussed the analysis of the input inductor design. In the present paper, the authors have discussed (i) the fundamental circuit operation confirmation of the FCBC, (ii) the design method of an input inductor, and (iii) the relationship between the capacitance of the flying capacitor and the output voltage ripple.

The principal in designing the input inductor in terms of the inductance and inductor core volume was explained. As a result, the inductance and inductor core volume of the input inductor were reduced by approximately 25% and 35%, respectively. Moreover, the relationship between the capacitance of the flying capacitor and the output voltage ripple was clearly established mathematically and was confirmed by simulation and experimental results. The experimental results confirmed that the capacitance of the flying capacitor and the output voltage ripple are independent of each other. Moreover, the maximum efficiency of the prototype converter was 98.5% at an output power of 1 kW.

In the future, balancing of the flying capacitor voltage of the FCBC will be considered by applying appropriate control strategies.

References

(1) H. Keyhani and H.A. Toliyat: "Flying-capacitor boost converter", in Twenty-Seventh Annual IEEE Applied Power Electronics Conference and Exposition (APEC), 2012 (2012)

(2) Z. Fan, F.Z. Peng, and Q. Zhaoming: "Study of the multilevel converters in DC-DC applications", in IEEE 35th Annual Power Electronics Specialists Conference, 2004. PESC 04. 2004 (2004)

(3) Z. Fan, D. Lei, F.Z. Peng, *et al.*: "A new design method for high efficiency DC-DC converters with flying capacitor technology", in Twenty-First Annual IEEE Applied Power Electronics Conference and Exposition, 2006. APEC'06 (2006)

(4) J. Itoh, K. Matsuura, and K. Orikawa: "Reduction of a boost inductance using a switched capacitor DC-DC converter", in IEEE 8th International Conference on Power Electronics and ECCE Asia (ICPE & ECCE), 2011 (2011)

(5) J. Yungtaek and M.M. Jovanovic: "Interleaved Boost Converter With Intrinsic Voltage-Doubler Characteristic for Universal-Line PFC Front End", IEEE Transactions on Power Electronics. Vol.22, No.4, pp.1394–1401 (2007)

(6) Z. Junhong, L. Jih-Sheng, K. Rae-young, *et al.*: "High-Power Density Design of a Soft-Switching High-Power Bidirectional dc-dc Converter", IEEE Transactions on Power Electronics, Vol.22, No.4, pp.1145–1153 (2007)

(7) G.V. Torrico-Bascope and I. Barbi: "A single phase PFC 3 kW converter using a three-state switching cell", in IEEE 35th Annual Power Electronics Specialists Conference, 2004. PESC 04. 2004 (2004)

(8) M. Hirakawa, Y. Watanabe, M. Nagano, *et al.*: "High power DC/DC converter using extreme close-coupled inductors aimed for electric vehicles", in International Power Electronics Conference (IPEC), 2010 (2010)

(9) S.Y. Tseng, J.Z. Shiang, H.H. Chang, *et al.*: "A Novel Turn-On/Off Snubber for Interleaved Boost Converters", in IEEE Power Electronics Specialists Conference, 2007. PESC 2007 (2007)

(10) Q. Dongyuan, Z. Bo, and Z. Chunfang: "Duty ratio control of resonant switched capacitor DC-DC converter", in Proceedings of the Eighth International Conference on Electrical Machines and Systems, 2005. ICEMS 2005 (2005)

(11) F.H. Khan and L.M. Tolbert: "A Multilevel Modular Capacitor Clamped DC-DC Converter", in 41st IAS Annual Meeting Conference Record of the 2006 IEEE Industry Applications Conference, 2006 (2006)

(12) O. Keiser, P.K. Steimer, and J.W. Kolar: "High power resonant Switched-Capacitor step-down converter", in IEEE Power Electronics Specialists Conference, 2008. PESC 2008 (2008)

(13) Z. Fan, D. Lei, P.F. Zheng, *et al.*: "A New Design Method for High-Power High-Efficiency Switched-Capacitor DC-DC Converters", IEEE Transactions on Power Electronics, Vol.23, No.2, pp.832–840 (2008)

(14) M. Shoyama and T. Ninomiya: "Output Voltage Control of Resonant Boost Switched Capacitor Converter", in Power Conversion Conference-Nagoya, 2007. PCC'07 (2007)

(15) D.W. Hart, *Power Electronics* 2011, New York: The McGraw-Hill Companies, Inc.

(16) N. Mohan, T.M. Undeland, and W.P. Robbins: *Power Electronics: Converters, Applications and Design*. Vol.3. 2003, United State of America: John Wiley & Sons, Inc.

(17) Wm.T. Mclyman: *Transformer and inductor design handbook*. 3rd. ed. 2004: Marcel Dekker, Inc.

(18) S.H. Hosseini, A.K. Sadig, and A. Sharifi: "Estimation of flying capacitors

voltages in multicell converters", in 6th International Conference on Electrical Engineering/Electronics, Computer, Telecommunications and Information Technology, 2009. ECTI-CON 2009 (2009)
(19) R. Bensaid and M. Fadel: "Flying capacitor voltages estimation in three-cell converters using a discrete-time Kalman filter at one third switching period", in Proceedings of the American Control Conference, 2002 (2002)
(20) G. Gateau, M. Fadel, P. Maussion, et al.: "Multicell converters: active control and observation of flying-capacitor voltages", IEEE Transactions on Industrial Electronics, Vol.49, No.5, pp.998–1008 (2002)

Asmarashid Bin Ponniran (Student Member) received his Bachelor Degree in Electrical Engineering and Master Degree in Electrical Engineering (Power) from Universiti Tun Hussein Onn Malaysia in 2002 and Universiti Teknologi Malaysia in 2005, respectively. Presently he is a Ph.D. candidate at Nagaoka University of Technology, Japan. At the same time, he is attached at Universiti Tun Hussein Onn Malaysia, Malaysia as a lecturer. His research interest includes dc-dc converter and its application.

Koichi Matsuura (Non-member) received the M.S. degree in electrical, electronics and information engineering from Nagaoka University of Technology, Nagaoka, Japan, in 2011. Since 2011, he has been an employee of Toyota Industries Corporation. His research interests include DC-DC converters.

Koji Orikawa (Member) received the M.S. and Ph.D. degrees in electrical, electronics and information engineering from Nagaoka University of Technology, Niigata, Japan, in 2010 and 2013 respectively. Since 2013, he has been working at Nagaoka University of Technology as a postdoctoral fellowship. He is the member of IEEE and IEEJ. His research interests include power conversion system especially DC-DC converters and high frequency techniques for power converters.

Jun-ichi Itoh (Member) received his M.S. and Ph.D. degrees in electrical and electronic systems engineering from Nagaoka University of Technology, Niigata, Japan in 1996 and 2000, respectively. From 1996 to 2004, he was with Fuji Electric Corporate Research and Development Ltd., Tokyo, Japan. Since 2004, He has been with Nagaoka University of Technology as an associate professor. He received the IEEJ Academic Promotion Award (IEEJ Technical Development Award) in 2007 and the Isao Takahashi Power Electronics Award in 2010. His research interests include matrix converters, DC/DC converters, power factor correction techniques and motor drives. He is a member of the Institute of Electrical Engineers of Japan and the Society of Automotive Engineers of Japan.